IEEE Access
Multidisciplinary : Rapid Review : Open Access Journal

Received December 10, 2019, accepted December 25, 2019, date of publication December 30, 2019, date of current version January 21, 2020.

Digital Object Identifier 10.1109/ACCESS.2019.2962811

Closed Form Solution for 3D Localization Based on Joint RSS and AOA Measurements for Mobile Communications

WANCHUN LI[1], **LI WANG**[1], **MANLIN XIAO**[2], **YINGXIANG LI**[3], **AND HUAGUO ZHANG**[1]

[1]School of Information and Communication Engineering, University of Electronic Science and Technology of China, Chengdu 611731, China
[2]Department of Urban Railway Transportation, Shanghai University of Engineering Science, Shanghai 201620, China
[3]School of Communication Engineering, Chengdu University of Information Technology, Chengdu 610225, China

Corresponding author: Wanchun Li (liwanchun@uestc.edu.cn)

This work was supported in part by the National Natural Science Foundation of China under Grant 61971103, and in part by the Meteorological information and Signal Processing Key Laboratory of Sichuan Higher Education Institutes, China.

ABSTRACT To address three-dimensional (3D) localization problems in the wireless sensor networks (WSNs) of mobile communications, a closed-form algorithm by utilizing hybrid information extracted from the received-signal-strength (RSS) with unknown signal powers and the angle-of-arrival (AOA) is proposed in this paper. Firstly, the distance of the target is expressed as the linear equation with respect to coordinates of target and trigonometric functions of angles. Then, the RSS measurement is rewritten as the ratios of distances between the target and different receiving sensors. Furthermore, the set of pseudo-linear equations for the location of target is derived with respect to the AOA and nonlinear RSS measurements. Under the condition of the small variance of measurements, the first-order Taylor expansion around the value of measurement is taken to the set of pseudo-linear equations and the first-order perturbation errors is also obtained. Finally, the solution of the target localization is derived utilizing the weighted least square (WLS). Theoretical analysis and simulation results show that the performance of proposed algorithm converge to the CRLB in the situation of the moderate measurement errors.

INDEX TERMS Localization, angle of arrival, received signal strength, closed-form solution.

I. INTRODUCTION

The passive localization of an emitter, in which multiple sensors are used to receive signals and the AOA [1]–[3], time difference of arrival (TDOA) [4] and RSS [5]–[8] extracted from the signals are utilized to estimate the location, has been applied in many fields such as radars, communications, surveillances, geological prospecting and global position systems (GPS). The target localization with unknown signal power is dependent on the information extracted from the TDOA, RSS and AOA measurements. The joint localization algorithms depend on RSS and AOA were discussed in paper [9]–[12]. This paper aims to locate the target using hybrid RSS and AOA measurements with unknown signal power.

The AOA localization algorithm, also known as the triangulation localization, is actually about the intersection localization problem of the spatial straight line from sensors to the target [1], [2]. The paper [3] discussed the AOA localization algorithm in analytic expression, in which the pseudo-linear equation of the target location is expressed by angles.

The target localization algorithm based on RSS that the location was estimated by measuring the multiple sensors' receiving signal powers emitted from the same target [5], [6], is classified into two types according to whether the emitting power is known. Two steps WLS estimation was proposed in paper [5], and the estimation algorithm based on semidefinite programming (SDP) was presented in [6]. These algorithms could reach the CRLB with high SNR. The location also can be calculated based on RSS measurement with unknown transmit power and path loss exponent [7], [8].

For the localization with hybrid RSS and AOA measurements [9]–[12], Chan *et al.* [9] proposed a 2WLS localization algorithm with intermediate variables. In his approach, the set of nonlinear equations for the hybrid RSS and AOA measurements with respect to the target location was rewritten

The associate editor coordinating the review of this manuscript and approving it for publication was Qingchun Chen.

as a set of linear equations for the intermediate variable in regard to the location so that the initial solution could be derived with WLS estimation. Furthermore, the constraint condition between the intermediate variable and the target location was utilized to obtain the final WLS localization solution. Through introducing a distance parameter, Tomic *et al.* [10] transformed the estimation problem with hybrid RSS and AOA measurements into a convex problem by applying appropriate SDP relaxation techniques. The localization could be realized by the convex optimization algorithm. And this approach was robust under the condition of unknown emitting power, but its computational complexity was high.

In the recent literature of Tomic *et al.* [11], a closed form WLS was presented. Since only errors of RSS were considered when using weight values, the accuracy of localization was unable to reach the CRLB even with minor angular measurement error. With the distance from the target to each receiver as the intermediate variable, the paper utilized SDP to obtain the localization solution. The estimation accuracy is enhanced, but it still has high computational complexity. In literature [12], Khan presented a closed-form solution with RSS and AOA measurements, but it was used in the 2D sense and cannot be used in the case of unknown transmit power. The paper [13] proposed a novel localization method based on RSS+AOA combined measurements by using polarized identity in 3D WSNs. The proposed scheme can work effectively in both cases of known and unknown target transmit power. And in literature [14], Slavisa Tomic addressed the problem of simultaneous localization of multiple targets in 3D cooperative WSNs by linearizing the measurement models and formulating a sub-optimal estimator. But both of them were not weighted strictly according to optimal weights, so they are hard to reach the CRLB. By using novel error approximate expressions for both RSS and AOA measurement models, new estimators based on the least squares (LS) criterion were proposed in paper [15]. But these estimators would be transformed into mixed SDP, so its computational complexity is high. And we can see from figure 7 in reference [15], this method also failed to reach the CRLB.

Inspired by [9], the first-order perturbing term with respect to the ratio of distance is firstly derived by taking first-order Taylor expansion in RSS measurement equations in this paper. Utilizing the priori information of AOA, the distance is expressed as a linear combination of sensors position and the target position, then, the nonlinear AOA measurement equations were rewritten as the set of linear equations with reference to the target location using the pseudo linear method. The set of nonlinear equations of hybrid AOA and RSS measurements about target location could be transformed to be linear equations and first-order perturbing term about the measurement errors of RSS and AOA without any intermediate variable, the closed-form solution could be derived by WLS which is weighted according to the variance of the first-order perturbing term. In the presence of moderate measurement noise, the proposed method can converge to the CRLB. In addition, the algorithm does not need the initial value and iterations to reach a desired result. Thus, the computational complexity is low.

The rest of this paper is structured as follows. The RSS and AOA measurement models are introduced in Section II. Section III describes the derivation of the proposed estimators in the case of cooperative localization with unknown emitting power and the performance analysis for proposed method. The simulation results and the computational complexity are shown in Section IV. Finally, Section V summarizes the main conclusions of this paper.

In this paper, italics represent scalars, lowercase boldface represents vectors, uppercase boldface represents matrices, and $\mathbb{R}^{M\times N}$represents the real matrix of M rows and N columns. diag $(\boldsymbol{a})$ is a diagonal matrix with the diagonal elements of $\boldsymbol{a}$. The operator $(\cdot)^T$ denotes the matrix/vector transpose and the operator $\boldsymbol{A}^{-1}$ denotes the inverse of a square matrix $\boldsymbol{A}$.

II. PROBLEM FORMULATION

Assuming the unknown location of the target is denoted by $\boldsymbol{x} = (x, y, z)^T$, K sensors are settled at the known locations $\boldsymbol{x}_k = (x_k, y_k, z_k)^T$, $k = 1, 2, \cdots, K$.

A. ANGLE MEASUREMENTS

The azimuth angle measurement θ_k from the target to the *kth* sensor could be expressed as

$$\begin{aligned} \theta_k &= \theta_k^0 + n_k^\theta \\ \theta_k^0 &= \tan^{-1}\left[(y - y_k) / (x - x_k)\right] \end{aligned} \tag{1}$$

where θ_k^0 is the true azimuth angle from the target to the *kth* sensor, n_k^θ follows zero-mean Gaussian distribution with variance σ_θ^2, denoted by $n_k^\theta \sim N\left(0, \sigma_\theta^2\right)$. Assuming measurement noise of each sensor is uncorrelated, define the noise vector as $\boldsymbol{n}^\theta = \left[n_1^\theta, n_2^\theta, \cdots, n_K^\theta\right]^T$, and then we have $E\left(\boldsymbol{n}^\theta\right) = \boldsymbol{0}$ and $E\left(\left(\boldsymbol{n}^\theta\right)\left(\boldsymbol{n}^\theta\right)^T\right) = \sigma_\theta^2 \boldsymbol{I}$.

The elevation angle measurement φ_k from the target to the *kth* sensor could be formulated as

$$\begin{aligned} \varphi_k &= \varphi_k^0 + n_k^\varphi \\ \varphi_k^0 &= \tan^{-1}\left[(z - z_k) / \sqrt{(x - x_k)^2 + (y - y_k)^2}\right] \end{aligned} \tag{2}$$

where φ_k^0 is the true elevation angle from the target to the *kth* sensor, n_k^φ follows zero-mean Gaussian distribution with variance σ_φ^2, denoted by $n_k^\varphi \sim N\left(0, \sigma_\varphi^2\right)$. Assuming measurement noise of each sensor is uncorrelated, define the noise vector as $\boldsymbol{n}^\varphi = \left[n_1^\varphi, n_2^\varphi, \cdots, n_K^\varphi\right]^T$, and then we have $E\left(\boldsymbol{n}^\varphi\right) = \boldsymbol{0}$ and $E\left(\left(\boldsymbol{n}^\varphi\right)\left(\boldsymbol{n}^\varphi\right)^T\right) = \sigma_\varphi^2 \boldsymbol{I}$.

B. RECEIVED SIGNAL STREGTH MEASUREMENTS

The receiving approach of RSS is shown in literature [5]. Assuming the power P_k received by the *kth* sensor is expressed as

$$P_k = \eta_0 d_k^{-\alpha} 10^{n_k^\beta/10} \quad k = 1, 2, \cdots, K \tag{3}$$

where η_0 is the unknown emitting source power, d_k is the distance between the kth sensor and the target, α is a priori path loss parameter (PPLP), taken 2∼6 in general and 2 in free space, n_k^β is independent identical distribution (i.i.d.) Gaussian noise with zero mean and variance σ_s^2. To make σ_s^2 as small as possible, the received power P_k could be equal to the average value of several measurements, as shown in [9].

To erase the effect of η_0 on localization algorithm, (3) is rewritten as

$$\frac{d_k}{d_1}=\left(\frac{P_k}{P_1}\right)^{\frac{1}{\alpha}} exp\left\{\frac{\left(n_k^\beta-n_1^\beta\right)(\ln 10)}{(10\alpha)}\right\} \quad k=2,3,\cdots,K \tag{4}$$

When the value of $n_k^\beta - n_1^\beta$ is small, according to literature [7],

$$exp\left\{\left(n_k^\beta-n_1^\beta\right)(\ln 10)/(10\alpha)\right\} = 1+\left(n_k^\beta-n_1^\beta\right)(\ln 10)/(10\alpha) \tag{5}$$

Define the normalized power ratio β_{1k} and the normalized constant ξ respectively as

$$\beta_{1k}=(P_k/P_1)^{1/\alpha} \quad \xi=(\ln 10)/(10\alpha) \tag{6}$$

Then, (5) could be replaced by

$$d_k/d_1=\beta_{1k}+\beta_{1k}\xi\left(n_k^\beta-n_1^\beta\right) \quad k=2,3,\cdots,K$$

When the measurement noise is zero, the distance d_k^0 from the target to the kth sensor is equal to the distance d_1^0 from the target to the $1th$ sensor multiplied by the normalized power ratio β_{1k}^0, i.e.

$$d_k^0=d_1^0\beta_{1k}^0 \quad k=2,3,\cdots,K \tag{7}$$

III. LOCALIZATION ALGORITHM

A. PSEUDO LINEARIZATION OF NONLINEAR ANGLE MEASUREMENT

The equation of azimuth and elevation angle is pseudo linearized and the following equation is obtained [3]

$$\begin{aligned}\sin\theta_k^0(x-x_k) &= \cos\theta_k^0(y-y_k)\times(x-x_k)\sin\varphi_k^0\cos\theta_k^0 \\ &\quad +(y-y_k)\sin\varphi_k^0\sin\theta_k^0 \\ &= (z-z_k)\cos\varphi_k^0\end{aligned} \tag{8}$$

B. PSEUDO LINEARIZATION OF DISTANCE REPRESENTATION

Fig. 1 demonstrates the geometrical relationships between the distances from kth sensor to the target $d_k^0, k=0,1,\cdots,K$ and their projections $r_k, z-z_k, x-x_k, y-y_k$ on the XOY plane, the ZOY plane, the X axis and the Y axis respectively, which could be expressed as follows.

$$\begin{aligned} d_k^0\cos\varphi_k^0\cos\theta_k^0 &= x-x_k \\ d_k^0\cos\varphi_k^0\sin\theta_k^0 &= y-y_k \\ d_k^0\sin\varphi_k^0 &= z-z_k\end{aligned} \tag{9}$$

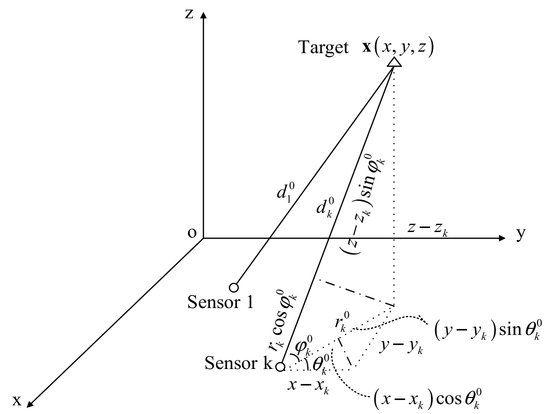

FIGURE 1. Schematic diagram of geometric relationship between angle and distance in 3D space.

As shown in Fig. 1, the distance from the kth sensor to the target d_k^0 could be denoted by

$$d_k^0=(x-x_k)\cos\varphi_k^0\cos\theta_k^0+(y-y_k)\cos\varphi_k^0\sin\theta_k^0 + (z-z_k)\sin\varphi_k^0 \tag{10}$$

Furthermore, applying (10) in (8), the linear equation of RSS with respect to the distances and angle measurements is derived as

$$\begin{aligned}&\beta_{1k}^0(x-x_1)\cos\varphi_1^0\cos\theta_1^0+\beta_{1k}^0(y-y_1)\cos\varphi_1^0\sin\theta_1^0 \\ &\quad+\beta_{1k}^0(z-z_1)\sin\varphi_1^0 \\ &\quad=(x-x_k)\cos\varphi_k^0\cos\theta_k^0+(y-y_k)\cos\varphi_k^0\sin\theta_k^0 \\ &\quad+(z-z_k)\sin\varphi_k^0\end{aligned} \tag{11}$$

C. DERIVATION OF LINEAR EQUATIONS

The measurements can be expressed as the set of linear equations with respect to the location of the target, according to (9), (12), shown in matrix form as

$$\boldsymbol{Ax}-\boldsymbol{b}=\boldsymbol{0} \tag{12}$$

where

$$\begin{aligned}&\boldsymbol{A}=\left[\boldsymbol{A}_\theta^T,\boldsymbol{A}_\varphi^T,\boldsymbol{A}_\beta^T\right]^T, \quad \boldsymbol{b}=\left[\boldsymbol{b}_\theta^T,\boldsymbol{b}_\varphi^T,\boldsymbol{b}_\beta^T\right]^T, \\ &\boldsymbol{A}_{\boldsymbol{\varphi}},\boldsymbol{A}_{\boldsymbol{\theta}}\in\mathbb{C}^{K\times 3}, \quad \boldsymbol{A}_{\boldsymbol{\beta}}\in\mathbb{C}^{(K-1)\times 3}, \\ &\boldsymbol{A}\in\mathbb{C}^{(3K-1)\times 3}, \quad \boldsymbol{b}\in\mathbb{C}^{(3K-1)\times 1}\end{aligned}$$

$$\boldsymbol{A}_\theta=\begin{bmatrix}\boldsymbol{a}_{\theta 1}\\ \vdots \\ \boldsymbol{a}_{\theta K}\end{bmatrix}\boldsymbol{A}_\varphi=\begin{bmatrix}\boldsymbol{a}_{\varphi 1}\\ \vdots \\ \boldsymbol{a}_{\varphi K}\end{bmatrix}\boldsymbol{A}_\beta=\begin{bmatrix}\boldsymbol{a}_{\beta 1}\\ \vdots \\ \boldsymbol{a}_{\beta K}\end{bmatrix}$$

$$\boldsymbol{a}_{\theta k}=\left[\sin\theta_k^0,-\cos\theta_k^0,0\right] \quad k=1,2,\cdots,K$$

$$\boldsymbol{a}_{\varphi k}=\left[\sin\varphi_k^0\cos\theta_k^0,\sin\varphi_k^0 sin\theta_k^0,\cos\varphi_k^0\right] \quad k=1,\cdots,K$$

$$\boldsymbol{a}_{\beta k}=\begin{bmatrix}\cos\varphi_k^0\cos\theta_k^0-\beta_{1k}^0\cos\varphi_1^0\cos\theta_1^0, \\ \cos\varphi_k^0\sin\theta_k^0-\beta_{1k}^0\cos\varphi_1^0\sin\theta_1^0, \\ \sin\varphi_k^0-\beta_{1k}^0\sin\varphi_1^0\end{bmatrix}$$
$$k=2,\cdots,K$$

$$\boldsymbol{b}_{\theta k}=x_k\sin\theta_k^0-y_k\cos\theta_k^0 \quad k=1,2,\cdots,K$$

$$
\begin{aligned}
\boldsymbol{b}_{\varphi k} &= x_k \sin\varphi_k^0 \cos\theta_k^0 + y_k \sin\varphi_k^0 \sin\theta_k^0 - z_k \cos\varphi_k^0 \\
&\quad k = 1, 2, \cdots, K \\
\boldsymbol{b}_{\beta k} &= x_k \cos\varphi_k^0 \cos\theta_k^0 + y_k \cos\varphi_k^0 \sin\theta_k^0 + z_k \sin\varphi_k^0 \\
&\quad - \beta_{1k}^0 x_1 \cos\varphi_1^0 \cos\theta_1^0 - \beta_{1k}^0 y_1 \cos\varphi_1^0 \sin\theta_1^0 \\
&\quad - \beta_{1k}^0 z_1 \sin\varphi_1^0 \quad k = 2, \cdots, K
\end{aligned}
$$

The values of angles, distances and radial distances involved in (12) should be true. However, these true values can't be obtained in practical scenarios. The corresponding measurements are used to get the localization solution by LS, i.e.

$$
\hat{\boldsymbol{x}}_{LS} = \left(\boldsymbol{A}^T\boldsymbol{A}\right)^{-1}\boldsymbol{A}^T\boldsymbol{b} \tag{13}
$$

D. IMPROVED LOCALIZATION ALGORITHM

Since the measurement errors occur in all cases, the accurate solution cannot be obtained from (13). Therefore, the WLS is considered to improve the algorithm.

In the measurements of azimuth angle in (1) and elevation angle in (2), the true values of angles can be rewritten as

$$
\theta_k^0 = \theta_k - n_k^\theta \quad \varphi_k^0 = \varphi_k - n_k^\varphi \tag{14}
$$

Since the measurement errors are much less than the true value, the trigonometric function of the true value of angle can be expanded by the first-order Taylor expansion around the measured value of angle, and only first-order perturbation error is remained, that is.

$$
\begin{aligned}
\sin\theta_k^0 &\approx \sin\theta_k - \cos\theta_k n_k^\theta \\
\cos\theta_k^0 &\approx \cos\theta_k + \sin\theta_k n_k^\theta \\
\sin\varphi_k^0 &\approx \sin\varphi_k - \cos\varphi_k n_k^\varphi \\
\cos\varphi_k^0 &\approx \cos\varphi_k + \sin\varphi_k n_k^\varphi \\
\sin\varphi_k^0 \sin\theta_k^0 &\approx \sin\theta_k \sin\varphi_k - \cos\theta_k \sin\varphi_k n_k^\theta \\
&\quad - \cos\varphi_k \sin\theta_k n_k^\varphi \\
\cos\theta_k^0 \cos\varphi_k^0 &\approx \cos\theta_k \cos\varphi_k + \sin\theta_k \cos\varphi_k n_k^\theta \\
&\quad + \sin\varphi_k \cos\theta_k n_k^\varphi \\
\sin\varphi_k^0 \cos\theta_k^0 &\approx \sin\varphi_k \cos\theta_k - \cos\varphi_k \cos\theta_k n_k^\varphi \\
&\quad + \sin\theta_k \sin\varphi_k n_k^\theta \\
\cos\varphi_k^0 \sin\theta_k^0 &\approx \cos\varphi_k \sin\theta_k + \sin\varphi_k \cos\theta_k n_k^\varphi \\
&\quad - \cos\theta_k \cos\varphi_k n_k^\theta
\end{aligned}
$$

Furthermore, the relationship between the true value and the measured value of the RSS ratio is that

$$
\beta_{1k}^0 = \beta_{1k} - \beta_{1k}\left(n_k^\beta - n_1^\beta\right) \quad k = 2, \cdots, K \tag{15}
$$

Taking (14) and (15) into (12) and only keeping first-order perturbation error, the matrix expression is derived as

$$
\boldsymbol{A}\boldsymbol{x} - \boldsymbol{b} \approx \boldsymbol{\varepsilon} \tag{16}
$$

where $\boldsymbol{A}, \boldsymbol{b}, \boldsymbol{x}$ have the same meanings with the letter in (12), but use the measurements values of angles, distances and radial distances instead of the true value respectively.

The error vector is defined as $\boldsymbol{\varepsilon} = \left[\boldsymbol{\varepsilon}_\theta^T, \boldsymbol{\varepsilon}_\varphi^T, \boldsymbol{\varepsilon}_\beta^T\right]^T$, where $\boldsymbol{\varepsilon}_\theta$, $\boldsymbol{\varepsilon}_\varphi$ and $\boldsymbol{\varepsilon}_\beta$ are the first-order perturbation errors of azimuth angle, elevation angle and RSS ratio respectively. When using the measurements instead of the true values, the measurement error vector is defined as $\boldsymbol{n} = \left[\left(\boldsymbol{n}^\theta\right)^T, \left(\boldsymbol{n}^\varphi\right)^T, \left(\boldsymbol{n}^\beta\right)^T\right]^T \in \mathbb{R}^{(3K-1)\times 1}$

By analyzing the first-order perturbation in (12), we have

$$
\begin{aligned}
\boldsymbol{\varepsilon}_\theta &= \boldsymbol{C}_\theta \boldsymbol{n}^\theta, \boldsymbol{\varepsilon}_\varphi = \mathrm{blkdiag}\left(\boldsymbol{C}_{\varphi\theta}, \boldsymbol{C}_\varphi\right)\left[\left(\boldsymbol{n}^\theta\right)^T, \left(\boldsymbol{n}^\varphi\right)^T\right]^T \\
\boldsymbol{\varepsilon}_\beta &= \left[\boldsymbol{\varepsilon}_{\beta 2}, \cdots, \boldsymbol{\varepsilon}_{\beta K}\right]^T \\
&= \left[\boldsymbol{C}_{\beta\theta 1}, \boldsymbol{C}_{\beta\theta 2}, \boldsymbol{C}_{\beta\varphi 1}, \boldsymbol{C}_{\beta\varphi 2}, \boldsymbol{C}_{\beta 1}, \boldsymbol{C}_{\beta 2}\right]\boldsymbol{n}
\end{aligned} \tag{17}
$$

where

$$
\begin{aligned}
\boldsymbol{C}_\theta &= \mathrm{diag}\left\{\cdots, (x - x_k)\cos\theta_k + (y - y_k)\sin\theta_k, \cdots\right\} \\
&\quad \in \mathbb{R}^{K\times K} \\
\boldsymbol{C}_{\varphi\theta} &= \mathrm{diag}\left\{\cdots, -(x - x_k)\sin\varphi_k \sin\theta_k + (y - y_k)\right. \\
&\quad \left.\times \sin\varphi_k \cos\theta_k, \cdots\right\} \in \mathbb{R}^{K\times K} \\
\boldsymbol{C}_\varphi &= \mathrm{diag}\left\{\cdots, (x - x_k)\cos\varphi_k \cos\theta_k + (y - y_k)\cos\varphi_k\right. \\
&\quad \left.\times \sin\theta_k + (z - z_k)\sin\varphi_k, \cdots\right\} \in \mathbb{R}^{K\times K} \\
\boldsymbol{\varepsilon}_{\beta k} &= \left[(y - y_k)\cos\varphi_k \cos\theta_k - (x - x_k)\cos\varphi_k \sin\theta_k\right] n_k^\theta \\
&\quad + \left[(z - z_k)\cos\varphi_k - (y - y_k)\sin\varphi_k \sin\theta_k - (x - x_k)\right. \\
&\quad \left.\times \sin\varphi_k \cos\theta_k\right] n_k^\varphi + \beta_{1k}\xi\left[(z - z_1)\sin\varphi_1\right. \\
&\quad \left. + (x - x_1)\cos\varphi_1 \cos\theta_1 + (y - y_1)\cos\varphi_1 \sin\theta_1\right] \\
&\quad \times \left(n_k^\beta - n_1^\beta\right) + \beta_{1k}\left[(x - x_1)\cos\varphi_1 \sin\theta_1\right. \\
&\quad \left. + (y - y_1)\cos\varphi_1 \cos\theta_1\right] n_1^\theta + \beta_{1k}\left[(x - x_1)\sin\varphi_1\right. \\
&\quad \left.\times \cos\theta_1 + (y - y_1)\sin\varphi_1 \sin\theta_1 - (z - z_1)\cos\varphi_1\right] n_1^\varphi
\end{aligned}
$$

Therefore, substituting (17) into (16), the error vector $\boldsymbol{\varepsilon}$ can be given as

$$
\boldsymbol{\varepsilon} = \begin{bmatrix} \boldsymbol{\varepsilon}_\theta \\ \boldsymbol{\varepsilon}_\varphi \\ \boldsymbol{\varepsilon}_\beta \end{bmatrix} = \boldsymbol{C}\boldsymbol{n} = \begin{bmatrix} \boldsymbol{C}_\theta & \boldsymbol{O} & \boldsymbol{O} \\ \boldsymbol{C}_{\varphi\theta} & \boldsymbol{C}_\varphi & \boldsymbol{O} \\ \boldsymbol{C}_{\beta\theta} & \boldsymbol{C}_{\beta\varphi} & \boldsymbol{C}_\beta \end{bmatrix} \begin{bmatrix} \boldsymbol{n}^\theta \\ \boldsymbol{n}^\varphi \\ \boldsymbol{n}^\beta \end{bmatrix} \tag{18}
$$

Assuming the measurement error vector has the following statistical property

$$
\mathbb{E}(\boldsymbol{n}) = \boldsymbol{0} \tag{19}
$$

$$
\mathbb{E}\left(\boldsymbol{n}\boldsymbol{n}^T\right) = \boldsymbol{W} = \mathrm{blkdiag}\left(\sigma_\theta^2\boldsymbol{I}, \sigma_\varphi^2\boldsymbol{I}, \sigma_s^2\boldsymbol{I}\right) \tag{20}
$$

where, $\mathrm{blkdiag}(\boldsymbol{A}, \boldsymbol{B})$ is a block diagonal matrix with the matrix $\boldsymbol{A}$ and the matrix $\boldsymbol{B}$ as elements.

Obviously, we have the statistical property of the first-order linear perturbation entry as follow,

$$
\mathbb{E}(\boldsymbol{\varepsilon}) = \boldsymbol{0} \tag{21}
$$

$$
\mathbb{E}\left(\boldsymbol{\varepsilon}\boldsymbol{\varepsilon}^T\right) = \boldsymbol{Q} = \boldsymbol{C}\mathbb{E}\left(\boldsymbol{n}\boldsymbol{n}^T\right)\boldsymbol{C}^T = \boldsymbol{C}\boldsymbol{W}\boldsymbol{C}^T \tag{22}
$$

Then, the WLS solution, equivalent BLUE (Best Linear Unbiased Estimator [16]) solution, can be obtained, i.e.,

$$
\hat{x}_{WLS} = \left(\boldsymbol{A}^T\boldsymbol{Q}^{-1}\boldsymbol{A}\right)^{-1}\boldsymbol{A}^T\boldsymbol{Q}^{-1}\boldsymbol{b} \tag{23}
$$

The target localization algorithm flow with AOA and RSS measurements is expressed in Table 1.

TABLE 1. Localization algorithm with AOA and RSS measurements.

Step 1: Setting the initial solution $\hat{\boldsymbol{x}}_{LS}$ with AOA and RSS measurements by (13);
Step2: Calculating the weight matrix $\boldsymbol{C}$ with the initial solution $\hat{\boldsymbol{x}}_{LS}$ by (18);
Step3: Expressing the statistical property of the first-order linear perturbation with the weight matrix $\boldsymbol{C}$ and the statistical property of the measurement error $\boldsymbol{W}$ by (22);
Step4: Obtaining the final localization solution by (23)

E. ASYMPTOTIC PERFORMANCE ANALYSIS

According to measurement models (1-3), we can obtain the theoretical accuracy bound of target position estimation as follows (the detailed derivation is discussed in the appendix A)

$$\mathbf{CRLB\_x} = \left[\sigma_\theta^{-2}\boldsymbol{H}_{\boldsymbol{x}}^{\boldsymbol{\theta}}\left(\boldsymbol{H}_{\boldsymbol{x}}^{\boldsymbol{\theta}}\right)^T + \sigma_\varphi^{-2}\boldsymbol{H}_{\boldsymbol{x}}^{\boldsymbol{\varphi}}\left(\boldsymbol{H}_{\boldsymbol{x}}^{\boldsymbol{\varphi}}\right)^T + \sigma_\beta^{-2}\boldsymbol{H}_{\boldsymbol{x}}^{\boldsymbol{\beta}}\left(\boldsymbol{I} - K^{-1}\mathbf{1}\mathbf{1}^T\right)\left(\boldsymbol{H}_{\boldsymbol{x}}^{\boldsymbol{\beta}}\right)^T\right]^{-1} \tag{24}$$

When the measurement error is small, the analysis is as follows:

From (16), the WLS can be easy obtained (see appendix B for details) [16]:

$$\mathbb{E}\left(\hat{\boldsymbol{x}}_{WLS} - \boldsymbol{x}\right) \approx \mathbf{0}$$
$$\mathbb{E}\left[\left(\hat{\boldsymbol{x}}_{WLS} - \boldsymbol{x}\right)\left(\hat{\boldsymbol{x}}_{WLS} - \boldsymbol{x}\right)^T\right] \approx \left(\boldsymbol{A}^T\boldsymbol{Q}^{-1}\boldsymbol{A}\right)^{-1} \tag{25}$$

Through detailed theoretical derivation(see appendix B for details)we can get:

$$\left(\boldsymbol{A}^T\boldsymbol{Q}^{-1}\boldsymbol{A}\right)^{-1} \approx \mathbf{CRLB\_x} \tag{26}$$

So, when the noise level is small, the performance of our proposed algorithm can approximate to the CRLB.

IV. SIMULATIONS

To illustrate the effectiveness of the proposed method, this section gives the performance comparison of Chan and SR_WLS algorithm under different AOA and RSS measurement error, PPLP and target location. The details are as follows.

A. THE PERFORMANCE ANALYSIS OF THE THREE LOCALIZATION ALGORITHMS WITH THE SAME MEASURING LOCATIONS AND THE DIFFERENT MEASUREMENT ERRORS

Simulation 1: The PPLP is expressed as α and the value is set to 3, the locations $\boldsymbol{x_r}$ of sensors are allocated at $[0, 1, 0.3;\ 0.5, 0.5, 0.3;\ 1, 0, 0.3;\ -0.5, 0.5, 0.3;\ 1, 0.3, 0.3;\ 1, -1, 0.3]$ *km*. The target location is at $(0, 0.5, 0)$ *km*, $\sigma_\theta = \sigma_\varphi = 1°$. The 10000 times Monte Carlo simulations results of several algorithms are shown in Fig. 2.3.4.

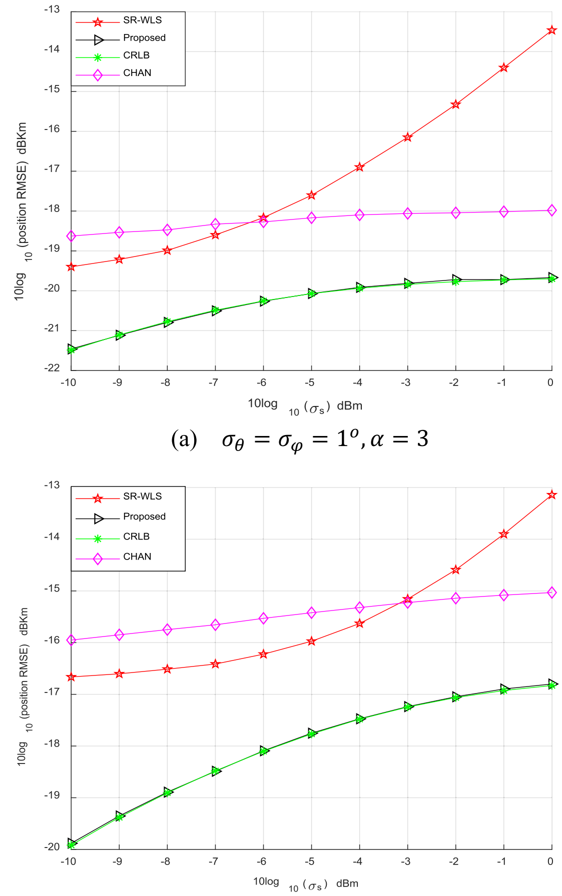

(a) $\sigma_\theta = \sigma_\varphi = 1^o, \alpha = 3$

(b) $\sigma_\theta = \sigma_\varphi = 2^o, \alpha = 3$

FIGURE 2. The RMSE of the target localization versus the variance of RSS with the same angle measurement errors.

As shown in above figures, the proposed WLS algorithm converges to the CRLB when the azimuth angle error and elevation angle error are both less than 1.5°. The performance of localization is gradually deviate from the CRLB as the measurement errors increase.

B. PERFORMANCE ANALYSIS FOR DIFFERENT NUMBER OF SENSORS

Simulation 2: the target location is at (0.5, 0.5, 0.5) km. The PPLP is expressed as α and the value is set to 3. The N sensors are allocated at the vertexes of an n-sided regular polygon with circumradius 1km on the XOY plane. The measurement errors are illustrated in each simulation. The results of 100000 times Monte Carlo simulations of several algorithms with different number of sensors are shown in Fig.5.

As shown in Fig.5, the accuracy of the proposed localization algorithm is improved and gets closer to the CRLB as the number of sensors increases.

C. LOCALIZATION ACCURACY ANALYSIS WITH DIFFERENT LOCATIONS OF TARGETS

Simulation 3: The angle measurement errors $\sigma_\theta = \sigma_\varphi = 1°$, the RSS measurement error $\sigma_s = 0.8dBm$, $\alpha = 3$, and the

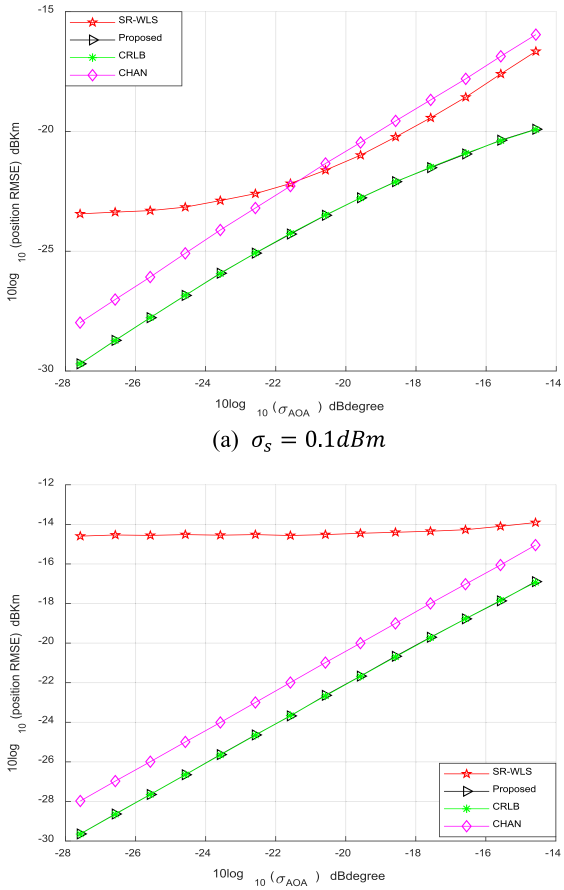

(a) $\sigma_s = 0.1dBm$

(b) $\sigma_s = 0.8dBm$

FIGURE 3. The RMSE of the target localization versus the variance of AOA with the same RSS measurement errors.

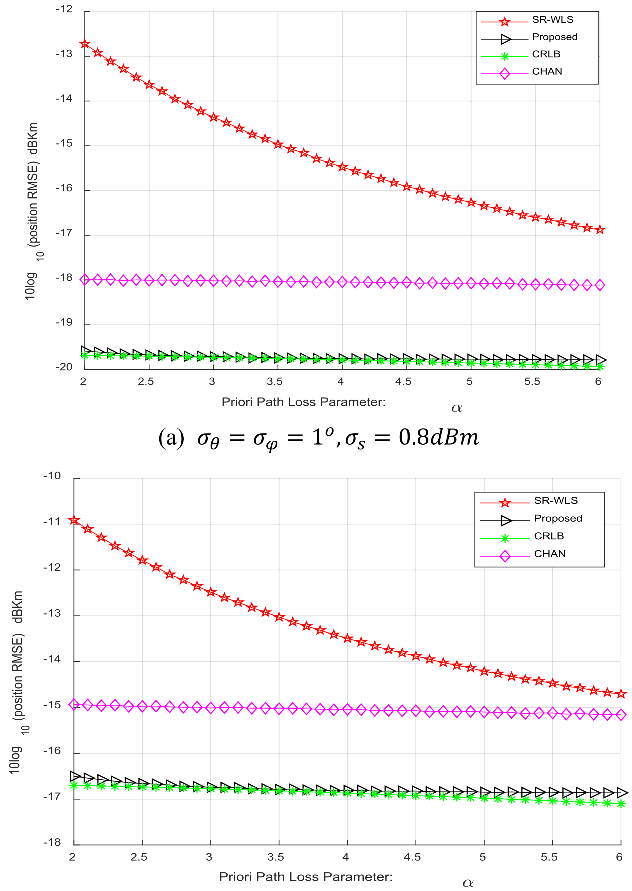

(a) $\sigma_\theta = \sigma_\varphi = 1^o, \sigma_s = 0.8dBm$

(b) $\sigma_\theta = \sigma_\varphi = 2^o, \sigma_s = 1.2dBm$

FIGURE 4. The RMSE of the target localization versus α with the same angle measurement errors and the same RSS measurement errors.

TABLE 2. Performance comparison of several algorithms with different target locations.

Target locations (km)	RMSE of localization (Km) LS	CHAN	SR-WLS	WLS	CRLB
(0.5,0.5,0.5)	0.0470	0.0185	0.0145	0.0138	0.0138
(-0.5,0.5,0.5)	0.0401	0.0186	0.0146	0.0139	0.0138
(0.5,-0.5,0.5)	0.0470	0.0186	0.0139	0.0137	0.0137
(0.5,0,0.5)	0.0417	0.0173	0.0148	0.0143	0.0143
(0,0.5,0.5)	0.0462	0.0173	0.0149	0.0146	0.0145
(0,-0.5,0.5)	0.0461	0.0173	0.0149	0.0145	0.0145
(-0.5,0,0.5)	0.0372	0.0174	0.0148	0.0144	0.0143

sensors are allocated at the vertexes of a regular hexagon with circumradius 1km on the XOY plane. The locations of target are shown in Table 2. And the locations of sensors and the speed of target are the same as the parameters in simulation 1.

As shown in Table 2, the RMSE of the proposed algorithm is very close to the CRLB wherever the target is when measurement error is not too high. The presented algorithm in this paper conducts strictly the weighted calculation according to residuals of the measurement errors but the algorithm proposed in [10] conducts the weighted calculation depended on the distances which are not the optimum weighted values. This is the reason why the presented algorithm is better than the algorithm proposed in [10].

D. COMPARISON OF CUMULATIVE DISTRIBUTION FUNCTION

In this case, the angle measurement error is 1° and other simulation parameters are the same as those in simulation 1. Fig.6.(a) and Fig.6.(b) show the CDFs of different localization algorithms under different RSS measurement errors. Comparing the cumulative distribution function (CDF) curves shown in Fig. 6 with 100000 times Monte Carlo simulations, we can see that the proposed algorithm has better localization performance than others.

E. COMPUTATIONAL COMPLEXITY ANALYSIS

Table 3 expresses the computational complexity of these algorithms which is mainly decided by the computation of matrix calculation in (18), weighted values matrix $\boldsymbol{Q}$ calculation and WLS calculation in (23).

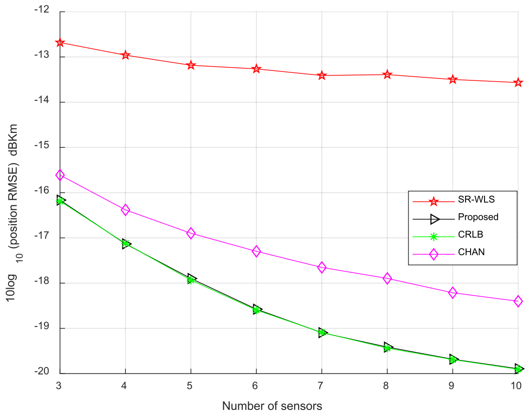

(a) $\sigma_\theta = \sigma_\varphi = 1^o, \sigma_s = 0.8dBm, \alpha = 3$

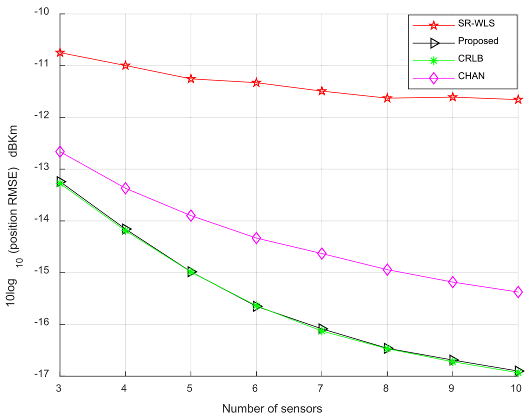

(b) $\sigma_\theta = \sigma_\varphi = 1^o, \sigma_s = 1.2dBm, \alpha = 3$

FIGURE 5. The RMSE of the target localization versus the different numbers of sensors.

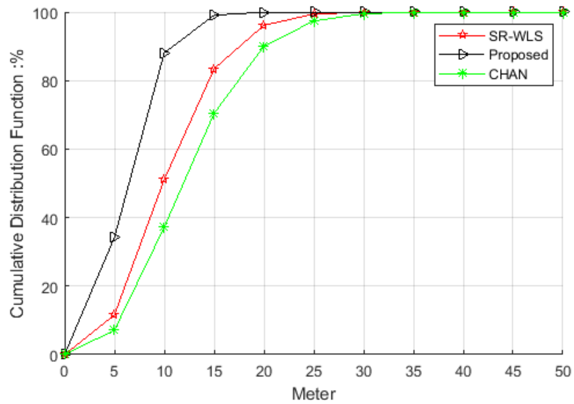

(a) $\sigma_s = 0.1dBm, \alpha = 3$

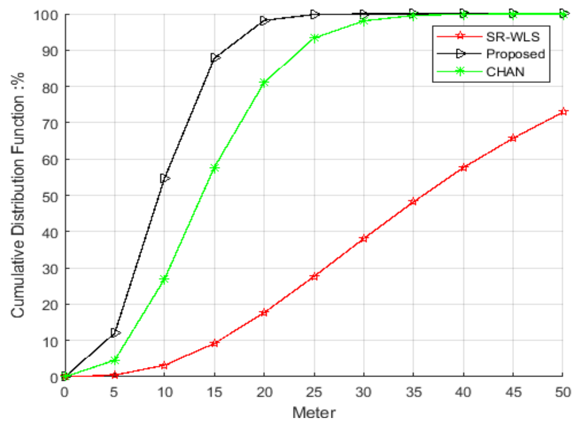

(b) $\sigma_s = 1dBm, \alpha = 3$

FIGURE 6. The CDFs of the different algorithms under different measurement errors.

TABLE 3. The computational complexities of three localization algorithms.

Algorithm	Description	Complexity
Chan	The WLS estimator for the non-cooperative localization when P_T is unknown in [9]	$O(K)$
SR-WLS	The SR-WLS estimator for the non-cooperative localization when P_T is unknown in [10]	$O(K_{max}K)$
Proposed	The WLS estimator for the non-cooperative localization when P_T is unknown in （23）	$O(K)$

As shown in Table 3, the computational complexity of the proposed algorithm has the same order of magnitude with the algorithm proposed by Chan and is less than the SR_WLS.

The simulation conditions are shown in Table 4. The computer CPU is Pentium (R) Dual-Core CPU E5800, the memory is 6GB, the operating system is win7, and the simulation software is matlab R2018a. Table 4 shows the time spent in running 100000 Monte Carlo experiments by various methods.

TABLE 4. The CPU running time of three localization algorithms.

Algorithm	CPU Running Time (second)
Chan	88.147 s
SR-WLS	352.618s
Proposed	78.652 s

From Table 4, we can see that the computation time of the proposed algorithm is slightly lower than that of Chan algorithm and far lower than that of SR-WLS algorithm, which proves the effectiveness of the proposed algorithm.

V. CONCLUSION

This paper proposed a closed-form analytical algorithm for the 3D localization using joint RSS and AOA measurements. This algorithm converts the complicated set of nonlinear equations with respect to measurements into the set of linear equations in regard to the location of the target. What's more, the closed-form localization is obtained by using the weighted LS. We can draw the conclusions according to the simulation results that the accuracy of the proposed algorithm is close to the CRLB when the angle measurement error is not too high. Therefore, we believe that this localization algorithm will be applied to the practical wireless communications field after further study.

APPENDIX

A. CRLB ANALYSIS

According to the statistical property of the measurement error (1) and (2), we have

$$\mathbb{E}\left(\boldsymbol{n}^{\theta}\left(\boldsymbol{n}^{\varphi}\right)^{T}\right)=\mathbb{E}\left(\boldsymbol{n}^{\theta}\left(\boldsymbol{n}^{\beta}\right)^{T}\right)=\mathbb{E}\left(\boldsymbol{n}^{\varphi}\left(\boldsymbol{n}^{\beta}\right)^{T}\right)=\boldsymbol{O}_{K\times K} \tag{A1}$$

where $\boldsymbol{O}_{K\times M}$ is an $K\times M$ matrix with all zero elements. (3) is rewritten as

$$n_k^{\beta}=10\left(\ln P_k-\alpha\ln d_k-\ln\eta_0\right)/\ln 10,\quad k=1,2,\cdots,K \tag{A2}$$

The set of all of the measurements is $\boldsymbol{\zeta}=\left[\boldsymbol{\theta}^T,\boldsymbol{\varphi}^T,\boldsymbol{\beta}^T\right]^T$, where $\boldsymbol{\theta}=[\theta_1,\cdots,\theta_K]^T$, $\boldsymbol{\beta}=\ln 10\,[\ln P_1,\cdots,\ln P_K]^T/10$, $\boldsymbol{\varphi}=[\varphi_1,\cdots,\varphi_K]^T$. By the statistical properties of the measurement errors in (A1) and (A2), the conditional probability can be expressed as

$$\begin{aligned}
&p\left(\boldsymbol{\zeta}|\boldsymbol{x},\eta_0\right)\\
&=const.*\exp\left\{-\frac{1}{2}\sigma_\theta^{-2}\left[\boldsymbol{\theta}-\boldsymbol{h}_{\boldsymbol{\theta}}(\boldsymbol{x})\right]^T\left[\boldsymbol{\theta}-\boldsymbol{h}_{\boldsymbol{\theta}}(\boldsymbol{x})\right]\right\}\\
&\quad*\exp\left\{-\frac{1}{2}\sigma_\varphi^{-2}\left[\boldsymbol{\varphi}-\boldsymbol{h}_{\boldsymbol{\varphi}}(\boldsymbol{x})\right]^T\left[\boldsymbol{\varphi}-\boldsymbol{h}_{\boldsymbol{\varphi}}(\boldsymbol{x})\right]\right\}\\
&\quad*\exp\left\{-\frac{1}{2}\sigma_\beta^{-2}\left[\boldsymbol{\beta}-\boldsymbol{h}_{\boldsymbol{\beta}}(\boldsymbol{x},\eta_0)\right]^T\left[\boldsymbol{\beta}-\boldsymbol{h}_{\boldsymbol{\beta}}(\boldsymbol{x},\eta_0)\right]\right\}
\end{aligned} \tag{A3}$$

where $const.=(2\pi)^{(-3K)/2}\,\sigma_\theta^{-K}\sigma_\varphi^{-K}\sigma_\beta^{-K}$ is a constant independent of the location parameter, and $(\boldsymbol{x},\eta_0)$ represent the location parameter and power to be estimated respectively. The measurement equations can be expressed as

$$\boldsymbol{h}_{\boldsymbol{\theta}}(\boldsymbol{x})=\begin{bmatrix}\arctan\left[(y-y_1)/(x-x_1)\right]\\ \vdots\\ \arctan\left[(y-y_K)/(x-x_K)\right]\end{bmatrix} \tag{A4}$$

$$\boldsymbol{h}_{\boldsymbol{\varphi}}(\boldsymbol{x})=\begin{bmatrix}\arctan\left[(z-z_1)/\sqrt{(x-x_1)^2+(y-y_1)^2}\right]\\ \vdots\\ \arctan\left[(z-z_K)/\sqrt{(x-x_K)^2+(y-y_K)^2}\right]\end{bmatrix} \tag{A5}$$

$$\boldsymbol{h}_{\boldsymbol{\beta}}(\boldsymbol{x},\eta_0)=\frac{10}{\ln 10}\begin{bmatrix}\alpha\ln d_1+\ln\eta_0\\ \vdots\\ \alpha\ln d_K+\ln\eta_0\end{bmatrix} \tag{A6}$$

Therefore, the Fisher matrix can be constructed by

$$FIM=\mathbf{H}\mathbf{Q}^{-1}\mathbf{H}^T \tag{A7}$$

where

$$\mathbf{H}=\frac{\partial\boldsymbol{\zeta}^T}{\partial\mathbf{x}}=\begin{bmatrix}\boldsymbol{H}_{\boldsymbol{x}}^{\boldsymbol{\theta}} & \boldsymbol{H}_{\boldsymbol{x}}^{\boldsymbol{\varphi}} & \boldsymbol{H}_{\boldsymbol{x}}^{\boldsymbol{\beta}}\\ \boldsymbol{O}_{1\times K} & \boldsymbol{O}_{1\times K} & \boldsymbol{H}_{\eta_0}^{\boldsymbol{\beta}}\end{bmatrix} \tag{A8}$$

$$\boldsymbol{Q}=\text{blkdiag}\left(\sigma_\theta^2\boldsymbol{I},\sigma_\varphi^2\boldsymbol{I},\sigma_\beta^2\boldsymbol{I}\right) \tag{A9}$$

$$\boldsymbol{H}_{\boldsymbol{x}}^{\boldsymbol{\theta}}=\frac{\partial\boldsymbol{h}_{\boldsymbol{\theta}}^T}{\partial\boldsymbol{x}}=\begin{bmatrix}-\dfrac{\sin\theta_1}{r_1} & \cdots & -\dfrac{\sin\theta_K}{r_K}\\ \dfrac{\cos\theta_1}{r_1} & \cdots & \dfrac{\cos\theta_K}{r_K}\\ 0 & \cdots & 0\end{bmatrix} \tag{A10}$$

$$\begin{aligned}\boldsymbol{H}_{\boldsymbol{x}}^{\boldsymbol{\varphi}}&=\frac{\partial\boldsymbol{h}_{\boldsymbol{\varphi}}^T}{\partial\boldsymbol{x}}\\
&=\begin{bmatrix}-\dfrac{\sin\varphi_1\cos\theta_1}{d_1} & \cdots & -\dfrac{\sin\varphi_K\cos\theta_K}{d_K}\\ -\dfrac{\sin\varphi_1\sin\theta_1}{d_1} & \cdots & -\dfrac{\sin\varphi_K\sin\theta_K}{d_K}\\ \dfrac{\cos\varphi_1}{d_1} & \cdots & \dfrac{\cos\varphi_K}{d_K}\end{bmatrix}\end{aligned} \tag{A11}$$

$$\begin{aligned}\boldsymbol{H}_{\boldsymbol{x}}^{\boldsymbol{\beta}}&=\frac{\partial\boldsymbol{h}_{\boldsymbol{\beta}}^T}{\partial\boldsymbol{x}}\\
&=\frac{10\alpha}{\ln 10}\begin{bmatrix}\dfrac{\cos\varphi_1\cos\theta_1}{d_1} & \cdots & \dfrac{\cos\varphi_K\cos\theta_K}{d_K}\\ \dfrac{\cos\varphi_1\sin\theta_1}{d_1} & \cdots & \dfrac{\cos\varphi_K\sin\theta_K}{d_K}\\ \dfrac{\sin\varphi_1}{d_1} & \cdots & \dfrac{\sin\varphi_K}{d_K}\end{bmatrix}\end{aligned} \tag{A12}$$

$$\boldsymbol{H}_{\eta_0}^{\boldsymbol{\beta}}=\frac{\partial\boldsymbol{h}_{\boldsymbol{\beta}}^T}{\partial\eta_0}=\frac{10}{\eta_0\ln 10}\begin{bmatrix}1 & \cdots & 1\end{bmatrix}=\frac{10}{\eta_0\ln 10}\mathbf{1}^T \tag{A13}$$

The CRLB of location parameters with respect to power is shown as

$$\mathbf{CRLB}=(\boldsymbol{FIM})^{-1} \tag{A14}$$

The CRLB of the localization is obtained from (A14), i.e.,

$$\mathbf{CRLB\_x}=\text{CRLB}\,(1:3,1:3) \tag{A15}$$

Substituting (A8), (A9) into (A7), yields:

$$\begin{aligned}&\mathbf{FIM}\\
&=\begin{bmatrix}\boldsymbol{H}_{\boldsymbol{x}}^{\boldsymbol{\theta}} & \boldsymbol{H}_{\boldsymbol{x}}^{\boldsymbol{\varphi}} & \boldsymbol{H}_{\boldsymbol{x}}^{\boldsymbol{\beta}}\\ \boldsymbol{O}_{1\times K} & \boldsymbol{O}_{1\times K} & \boldsymbol{H}_{\eta_0}^{\boldsymbol{\beta}}\end{bmatrix}\begin{bmatrix}\boldsymbol{\sigma}_{\boldsymbol{\theta}}^{-2}\boldsymbol{I} & & \\ & \boldsymbol{\sigma}_{\boldsymbol{\varphi}}^{-2}\boldsymbol{I} & \\ & & \boldsymbol{\sigma}_{\boldsymbol{\beta}}^{-2}\boldsymbol{I}\end{bmatrix}\\
&\quad\times\begin{bmatrix}\left(\boldsymbol{H}_{\boldsymbol{x}}^{\boldsymbol{\theta}}\right)^{\boldsymbol{T}} & \boldsymbol{O}_{\boldsymbol{K}\times 1}\\ \left(\boldsymbol{H}_{\boldsymbol{x}}^{\boldsymbol{\varphi}}\right)^{\boldsymbol{T}} & \boldsymbol{O}_{\boldsymbol{K}\times 1}\\ \left(\boldsymbol{H}_{\boldsymbol{x}}^{\boldsymbol{\beta}}\right)^{\boldsymbol{T}} & \left(\boldsymbol{H}_{\eta_0}^{\boldsymbol{\beta}}\right)^{\boldsymbol{T}}\end{bmatrix}\end{aligned}$$

$$= \begin{bmatrix} \boldsymbol{\Omega} & \sigma_\beta^{-2} H_x^\beta \left(H_{\eta 0}^\beta\right)^T \\ \sigma_\beta^{-2} H_{\eta 0}^\beta \left(H_x^\beta\right)^T & \sigma_\beta^{-2} H_{\eta 0}^\beta \left(H_{\eta 0}^\beta\right)^T \end{bmatrix} \tag{A16}$$

Here,

$$\boldsymbol{\Omega} = \sigma_\theta^{-2} H_x^\theta \left(H_x^\theta\right)^T + \sigma_\varphi^{-2} H_x^\varphi \left(H_x^\varphi\right)^T + \sigma_\beta^{-2} H_x^\beta \left(H_x^\beta\right)^T$$

Utilizing the matrix inversion formula [17]

$$\begin{bmatrix} A & b \\ b^T & \alpha \end{bmatrix}^{-1} = \begin{bmatrix} \left(A - \alpha^{-1} b b^T\right)^{-1} & -A^{-1} b \left(\alpha - b^T A^{-1} b\right)^{-1} \\ -\left(\alpha - b^T A^{-1} b\right)^{-1} b^T A^{-1} & \left(\alpha - b^T A^{-1} b\right)^{-1} \end{bmatrix} \tag{A17}$$

Substituting (A8), (A9) into (A17),

$$\mathbf{CRLB_x} = \Big[\sigma_\theta^{-2} H_x^\theta \left(H_x^\theta\right)^T + \sigma_\varphi^{-2} H_x^\varphi \left(H_x^\varphi\right)^T + \sigma_\beta^{-2} H_x^\beta \left(H_x^\beta\right)^T - \sigma_\beta^{-2} \left(H_{\eta_0}^\beta \left(H_{\eta_0}^\beta\right)^T\right)^{-1} H_x^\beta \left(H_{\eta_0}^\beta\right)^T H_{\eta_0}^\beta \left(H_x^\beta\right)^T\Big]^{-1} \tag{A18}$$

From (A13), we have

$$\left(H_{\eta_0}^\beta \left(H_{\eta_0}^\beta\right)^T\right)^{-1} = \frac{(\eta_0 ln10)^2}{100K} \tag{A19}$$

$$\left(H_{\eta_0}^\beta\right)^T H_{\eta_0}^\beta = \frac{100}{(\eta_0 ln10)^2} \mathbf{1}\mathbf{1}^T \tag{A20}$$

Substituting (A19), (A20) and (A13) into (A18), yields:

$$\mathbf{CRLB\_x} = \Big[\sigma_\theta^{-2} H_x^\theta \left(H_x^\theta\right)^T + \sigma_\varphi^{-2} H_x^\varphi \left(H_x^\varphi\right)^T + \sigma_\beta^{-2} H_x^\beta \left(H_x^\beta\right)^T - \sigma_\beta^{-2} K^{-1} H_x^\beta \mathbf{1}\mathbf{1}^T \left(H_x^\beta\right)^T\Big]^{-1}$$
$$= \Big[\sigma_\theta^{-2} H_x^\theta \left(H_x^\theta\right)^T + \sigma_\varphi^{-2} H_x^\varphi \left(H_x^\varphi\right)^T + \sigma_\beta^{-2} H_x^\beta \left(H_x^\beta\right)^T + \sigma_\beta^{-2} H_x^\beta \left(I - K^{-1}\mathbf{1}\mathbf{1}^T\right)\left(H_x^\beta\right)^T\Big]^{-1}$$

B. ASYMPTOTIC PERFORMANCE ANALYSIS

From (16) we can obtain the following optimization problem

$$\min_x \left\{(\mathbf{Ax} - \mathbf{b})^T \mathbf{Q}^{-1} (\mathbf{Ax} - \mathbf{b})\right\} \tag{B1}$$

where

$$Q = \mathbb{E}\left(\varepsilon \varepsilon^T\right) = C \mathbb{E}\left(n n^T\right) C^T = CWC^T$$

The weighted least squares solution is

$$\hat{x}_{WLS} = \left(A^T Q^{-1} A\right)^{-1} A^T Q^{-1} b \tag{B2}$$

So we have

$$\begin{aligned} \mathbb{E}\left(\hat{x}_{WLS} - x\right) &= \mathbb{E}\left(\left(A^T Q^{-1} A\right)^{-1} A^T Q^{-1} b - x\right) \\ &= \mathbb{E}\left(\left(A^T Q^{-1} A\right)^{-1} A^T Q^{-1} (Ax - \varepsilon) - x\right) \\ &= \mathbb{E}\left(\left(A^T Q^{-1} A\right)^{-1} A^T Q^{-1} \varepsilon\right) \approx \mathbf{0} \end{aligned} \tag{B3}$$

and

$$\begin{aligned} &\mathbb{E}\left[\left(\hat{x}_{WLS} - x\right)\left(\hat{x}_{WLS} - x\right)^T\right] \\ &= \mathbb{E}\left[\left(\left(A^T Q^{-1} A\right)^{-1} A^T Q^{-1} \varepsilon\right)\left(\left(A^T Q^{-1} A\right)^{-1} A^T Q^{-1} \varepsilon\right)^T\right] \\ &= \mathbb{E}\left[\left(A^T Q^{-1} A\right)^{-1} A^T Q^{-1} \varepsilon \varepsilon^T Q^{-1} A \left(A^T Q^{-1} A\right)^{-1}\right] \\ &= \left(A^T Q^{-1} A\right)^{-1} A^T Q^{-1} \mathbb{E}\left(\varepsilon \varepsilon^T\right) Q^{-1} A \left(A^T Q^{-1} A\right)^{-1} \\ &= \left(A^T Q^{-1} A\right)^{-1} A^T Q^{-1} Q Q^{-1} A \left(A^T Q^{-1} A\right)^{-1} \\ &\approx \left(A^T Q^{-1} A\right)^{-1} \end{aligned} \tag{B4}$$

When the measurement noise is small, from (17) we can get:

$$\begin{aligned} &(x - x_k)\cos\theta_k + (y - y_k)\sin\theta_k \\ &\quad \approx \left(x^0 - x_k\right)\cos\theta_k^0 + \left(y^0 - y_k\right)\sin\theta_k^0 \\ &\quad = r_k^0 \end{aligned} \tag{B5}$$

$$\begin{aligned} &-(x - x_k)\sin\varphi_k \sin\theta_k + (y - y_k)\sin\varphi_k \cos\theta_k \\ &\quad = \sin\varphi_k\left[-(x - x_k)\sin\theta_k + (y - y_k)\cos\theta_k\right] \\ &\quad \approx \sin\varphi_k\left[-r_k^0 \cos\theta_k^0 \sin\theta_k^0 + r_k^0 \cos\theta_k^0 \sin\theta_k^0\right] \\ &\quad = 0 \end{aligned} \tag{B6}$$

$$\begin{aligned} &(y - y_k)\cos\varphi_k \cos\theta_k - (x - x_k)\cos\varphi_k \sin\theta_k \\ &\quad = \cos\varphi_k\left[-(x - x_k)\sin\theta_k + (y - y_k)\cos\theta_k\right] \\ &\quad \approx \cos\varphi_k\left[-r_k^0 \cos\theta_k^0 \sin\theta_k^0 + r_k^0 \cos\theta_k^0 \sin\theta_k^0\right] \\ &\quad = 0 \end{aligned} \tag{B7}$$

Putting (B5) into (18), yield

$$C_\theta = diag\left\{r_1^0, \cdots, r_K^0\right\} \tag{B8}$$

Putting (B6) into (18), yield

$$C_{\varphi\theta} = O \tag{B9}$$

Putting (B7) into (18), yield

$$C_{\beta\theta} = O \tag{B10}$$

From (17), (18), matrix $\boldsymbol{C}_\beta$ can be rewrite as

$$\begin{aligned}\boldsymbol{C}_\beta &= \begin{bmatrix} -\boldsymbol{\beta}_{12}\boldsymbol{\xi d}_1 & \boldsymbol{\beta}_{12}\boldsymbol{\xi d}_1 & \cdots & \boldsymbol{0} \\ \vdots & \vdots & \ddots & \vdots \\ -\beta_{1K}\boldsymbol{\xi d}_1 & \boldsymbol{0} & \cdots & \boldsymbol{\beta}_{1K}\boldsymbol{\xi d}_1 \end{bmatrix} \\ &= \boldsymbol{\xi d}_1 \begin{bmatrix} \boldsymbol{\beta}_{12} & \cdots & \boldsymbol{0} \\ \vdots & \ddots & \vdots \\ \boldsymbol{0} & \cdots & \boldsymbol{\beta}_{1K} \end{bmatrix} \\ &\times \left[-\boldsymbol{1}_{(K-1)\times 1} \quad \boldsymbol{I}_{(K-1)\times(K-1)} \right] \end{aligned} \tag{B11}$$

Taking (B8-B11) into (18), yields

$$\boldsymbol{C} = \text{blkdiag}\left(\boldsymbol{C}_{\boldsymbol{\theta}}, \boldsymbol{C}_{\boldsymbol{\varphi}}, \boldsymbol{C}_{\boldsymbol{\beta}}\right) \tag{B12}$$

From (22), we can obtain:

$$\boldsymbol{Q} = \text{blkdiag}\left(\sigma_\theta^2 \boldsymbol{C}_{\boldsymbol{\theta}} \boldsymbol{C}_{\boldsymbol{\theta}}^T, \sigma_\varphi^2 \boldsymbol{C}_{\boldsymbol{\varphi}} \boldsymbol{C}_{\boldsymbol{\varphi}}^T, \sigma_\beta^2 \boldsymbol{C}_{\boldsymbol{\beta}} \boldsymbol{C}_{\boldsymbol{\beta}}^T\right) \tag{B13}$$

Putting (12), (B12) and (B13) into (18), yields

$$\begin{aligned}&\left(\boldsymbol{A}^T \boldsymbol{Q}^{-1} \boldsymbol{A}\right)^{-1} \\ &= \Big[\sigma_\theta^{-2} \boldsymbol{A}_{\boldsymbol{\theta}}^T \left(\boldsymbol{C}_{\boldsymbol{\theta}} \boldsymbol{C}_{\boldsymbol{\theta}}^T\right)^{-1} \boldsymbol{A}_{\boldsymbol{\theta}} \\ &\quad + \sigma_\varphi^{-2} \boldsymbol{A}_{\boldsymbol{\varphi}}^T \left(\boldsymbol{C}_{\boldsymbol{\varphi}} \boldsymbol{C}_{\boldsymbol{\varphi}}^T\right)^{-1} \boldsymbol{A}_{\boldsymbol{\varphi}} + \sigma_\beta^{-2} \boldsymbol{A}_{\boldsymbol{\beta}}^T \left(\boldsymbol{C}_{\boldsymbol{\beta}} \boldsymbol{C}_{\boldsymbol{\beta}}^T\right)^{-1} \boldsymbol{A}_{\boldsymbol{\beta}}\Big]^{-1}\end{aligned} \tag{B14}$$

The first term of the right side in (B14) can be calculated as

$$\begin{aligned}&\boldsymbol{A}_{\boldsymbol{\theta}}^T \left(\boldsymbol{C}_{\boldsymbol{\theta}} \boldsymbol{C}_{\boldsymbol{\theta}}^T\right)^{-1} \boldsymbol{A}_{\boldsymbol{\theta}} \\ &= \begin{bmatrix} \sin\theta_1^0, -\cos\theta_1^0, 0 \\ \vdots \\ \sin\theta_K^0, -\cos\theta_K^0, 0 \end{bmatrix}^T \begin{bmatrix} (r_1^0)^{-2} & \cdots & \\ \vdots & \ddots & \vdots \\ & \cdots & (r_K^0)^{-2} \end{bmatrix} \\ &\quad \times \begin{bmatrix} \sin\theta_1^0, -\cos\theta_1^0, 0 \\ \vdots \\ \sin\theta_K^0, -\cos\theta_K^0, 0 \end{bmatrix} \\ &= \begin{bmatrix} \frac{\sin\theta_1^0}{r_1^0}, -\cos\frac{\theta_1^0}{r_1^0}, 0 \\ \vdots \\ \frac{\sin\theta_K^0}{r_K^0}, -\frac{\cos\theta_K^0}{r_K^0}, 0 \end{bmatrix}^T \begin{bmatrix} \frac{\sin\theta_1^0}{r_1^0}, -\cos\frac{\theta_1^0}{r_1^0}, 0 \\ \vdots \\ \frac{\sin\theta_K^0}{r_K^0}, -\frac{\cos\theta_K^0}{r_K^0}, 0 \end{bmatrix} \\ &= \boldsymbol{H}_{\boldsymbol{x}}^{\boldsymbol{\theta}} \left(\boldsymbol{H}_{\boldsymbol{x}}^{\boldsymbol{\theta}}\right)^T\end{aligned} \tag{B15}$$

The second term of the right side in (B14) can be computed as

$$\begin{aligned}&\boldsymbol{A}_{\boldsymbol{\varphi}}^T \left(\boldsymbol{C}_{\boldsymbol{\varphi}} \boldsymbol{C}_{\boldsymbol{\varphi}}^T\right)^{-1} \boldsymbol{A}_{\boldsymbol{\varphi}} \\ &= \begin{bmatrix} \sin\varphi_1^0 \cos\theta_1^0, \sin\varphi_1^0 \sin\theta_1^0, \cos\varphi_1^0 \\ \vdots \\ \sin\varphi_K^0 \cos\theta_K^0, \sin\varphi_K^0 \sin\theta_K^0, \cos\varphi_K^0 \end{bmatrix}^T \\ &\quad \times \begin{bmatrix} (d_1^0)^{-2} & \cdots & \\ \vdots & \ddots & \vdots \\ & \cdots & (d_K^0)^{-2} \end{bmatrix} \\ &\quad \times \begin{bmatrix} \sin\varphi_1^0 \cos\theta_1^0, \sin\varphi_1^0 \sin\theta_1^0, \cos\varphi_1^0 \\ \vdots \\ \sin\varphi_K^0 \cos\theta_K^0, \sin\varphi_K^0 \sin\theta_K^0, \cos\varphi_K^0 \end{bmatrix} \\ &= \begin{bmatrix} \sin\varphi_1^0 \cos\theta_1^0/d_1^0, \sin\varphi_1^0 \sin\theta_1^0/d_1^0, \cos\varphi_1^0/d_1^0 \\ \vdots \\ \sin\varphi_K^0 \cos\theta_K^0/d_K^0, \sin\varphi_K^0 \sin\theta_K^0/d_K^0, \cos\varphi_K^0/d_K^0 \end{bmatrix}^T \\ &\quad \times \begin{bmatrix} \sin\varphi_1^0 \frac{\cos\theta_1^0}{d_1^0}, \frac{\sin\varphi_1^0 \sin\theta_1^0}{d_1^0}, \frac{\cos\varphi_1^0}{d_1^0} \\ \vdots \\ \sin\varphi_K^0 \frac{\cos\theta_K^0}{d_K^0}, \sin\varphi_K^0 \sin\frac{\theta_K^0}{d_K^0}, \frac{\cos\varphi_K^0}{d_K^0} \end{bmatrix} \\ &= \boldsymbol{H}_{\boldsymbol{x}}^{\boldsymbol{\varphi}} \left(\boldsymbol{H}_{\boldsymbol{x}}^{\boldsymbol{\varphi}}\right)^T\end{aligned} \tag{B16}$$

Let us denote $\boldsymbol{\Lambda}$ as

$$\boldsymbol{\Lambda} = \left[-\boldsymbol{1}_{(K-1)\times 1} \quad \boldsymbol{I}_{(K-1)\times(K-1)} \right] \in \mathbb{R}^{(K-1)\times K}$$

Utilizing the matrix inversion formula, yields

$$\begin{aligned}&\left(\boldsymbol{\Lambda}\boldsymbol{\Lambda}^T\right)^{-1} \\ &= \left(\boldsymbol{I}_{(K-1)\times(K-1)} + \boldsymbol{1}_{(K-1)\times 1} \boldsymbol{1}_{(K-1)\times 1}^T\right)^{-1} \\ &= \left(\boldsymbol{I}_{(K-1)\times(K-1)} - K^{-1} \boldsymbol{1}_{(K-1)\times 1} \boldsymbol{1}_{(K-1)\times 1}^T\right)\end{aligned} \tag{B17}$$

The third term of the right side in (B14) can be computed as

$$\begin{aligned}\boldsymbol{A}_\beta^T \boldsymbol{Q}_\beta^{-1} \boldsymbol{A}_\beta &= \sigma_\beta^{-2} \boldsymbol{A}_\beta^T \left(\boldsymbol{C}_\beta \boldsymbol{C}_{\boldsymbol{\beta}}^T\right)^{-1} \boldsymbol{A}_\beta \\ &= \sigma_\beta^{-2} \xi^{-2} d_1^{-2} \boldsymbol{A}_\beta^T \begin{bmatrix} \beta_{12}^{-1} & \cdots & \\ \vdots & \ddots & \vdots \\ & \cdots & \beta_{1K}^{-1} \end{bmatrix} \\ &\quad \times \left(\boldsymbol{\Lambda}\boldsymbol{\Lambda}^T\right)^{-1} \begin{bmatrix} \beta_{12}^{-1} & \cdots & \\ \vdots & \ddots & \vdots \\ & \cdots & \beta_{1K}^{-1} \end{bmatrix} \boldsymbol{A}_\beta \\ &= \sigma_\beta^{-2} \xi^{-2} \boldsymbol{A}_\beta^T \begin{bmatrix} d_2^{-1} & \cdots & \\ \vdots & \ddots & \vdots \\ & \cdots & d_K^{-1} \end{bmatrix} \\ &\quad \times \left(\boldsymbol{I}_{(K-1)\times(K-1)} - K^{-1} \boldsymbol{1}_{(K-1)\times 1} \boldsymbol{1}_{(K-1)\times 1}^T\right) \\ &\quad \times \begin{bmatrix} d_2^{-1} & \cdots & \\ \vdots & \ddots & \vdots \\ & \cdots & d_K^{-1} \end{bmatrix} \boldsymbol{A}_\beta\end{aligned} \tag{B18}$$

Note that

$$
\begin{aligned}
&\xi^{-1}\boldsymbol{A}_{\beta}^{T}\begin{bmatrix} d_2^{-1} & \cdots & \\ \vdots & \ddots & \vdots \\ & \cdots & d_K^{-1}\end{bmatrix} \\
&=\xi^{-1}\left\{\begin{bmatrix} d_2^{-1}\cos\varphi_2^0\cos\theta_2^0 & \cdots & d_K^{-1}\cos\varphi_K^0\cos\theta_K^0 \\ d_2^{-1}\cos\varphi_2^0\sin\theta_2^0 & \cdots & d_K^{-1}\cos\varphi_K^0\sin\theta_K^0 \\ d_2^{-1}\sin\varphi_2^0 & \cdots & d_K^{-1}\sin\varphi_K^0 \end{bmatrix}\right. \\
&\quad\left.-\begin{bmatrix} d_1^{-1}\cos\varphi_1^0\cos\theta_1^0 & \cdots & d_1^{-1}\cos\varphi_1^0\cos\theta_1^0 \\ d_1^{-1}\cos\varphi_1^0\sin\theta_1^0 & \cdots & d_1^{-1}\cos\varphi_1^0\sin\theta_1^0 \\ d_1^{-1}\sin\varphi_1^0 & \cdots & d_1^{-1}\sin\varphi_1^0 \end{bmatrix}\right\} \\
&=\xi^{-1}\begin{bmatrix} d_1^{-1}\cos\varphi_2^0\cos\theta_2^0 & \cdots & d_K^{-1}\cos\varphi_K^0\cos\theta_K^0 \\ d_1^{-1}\cos\varphi_2^0\sin\theta_2^0 & \cdots & d_K^{-1}\cos\varphi_K^0\sin\theta_K^0 \\ d_1^{-1}\sin\varphi_2^0 & \cdots & d_K^{-1}\sin\varphi_K^0 \end{bmatrix}\boldsymbol{\Lambda}^T \\
&=\boldsymbol{H}_{\boldsymbol{x}}^{\beta}\boldsymbol{\Lambda}^T
\end{aligned} \tag{B19}
$$

On the other hand

$$
\begin{aligned}
&\boldsymbol{\Lambda}^T\left(\boldsymbol{I}_{(K-1)\times(K-1)}-K^{-1}\mathbf{1}_{(K-1)\times 1}\mathbf{1}_{(K-1)\times 1}^T\right)\boldsymbol{\Lambda} \\
&=\begin{bmatrix} -\mathbf{1}_{(K-1)\times 1}^T \\ \boldsymbol{I}_{(K-1)\times(K-1)}\end{bmatrix} \\
&\quad\times\left(\boldsymbol{I}_{(K-1)\times(K-1)}-K^{-1}\mathbf{1}_{(K-1)\times 1}\mathbf{1}_{(K-1)\times 1}^T\right) \\
&\quad\times\begin{bmatrix} -\mathbf{1}_{(K-1)\times 1} & \boldsymbol{I}_{(K-1)\times(K-1)}\end{bmatrix} \\
&=\begin{bmatrix} -K^{-1}\mathbf{1}_{(K-1)\times 1}^T \\ \boldsymbol{I}_{(K-1)\times(K-1)}-K^{-1}\mathbf{1}_{(K-1)\times 1}\mathbf{1}_{(K-1)\times 1}^T\end{bmatrix} \\
&\quad\times\begin{bmatrix} -\mathbf{1}_{(K-1)\times 1} & \boldsymbol{I}_{(K-1)\times(K-1)}\end{bmatrix} \\
&=\frac{1}{K}\begin{bmatrix} K-1 & -\mathbf{1}_{(K-1)\times 1}^T \\ -\mathbf{1}_{(K-1)\times 1} & K\left(\boldsymbol{I}_{(K-1)\times(K-1)}-\mathbf{1}_{(K-1)\times 1}\mathbf{1}_{(K-1)\times 1}^T\right)\end{bmatrix} \\
&=\boldsymbol{I}_{K\times K}-K^{-1}\mathbf{1}_{K\times 1}\mathbf{1}_{K\times 1}^T
\end{aligned} \tag{B20}
$$

Putting (B19) and (B20) into (B18), yields

$$
\boldsymbol{A}_{\beta}^T\left(\boldsymbol{C}_{\beta}\boldsymbol{C}_{\beta}^T\right)^{-1}\boldsymbol{A}_{\beta}=\sigma_{\beta}^{-2}\boldsymbol{H}_{\boldsymbol{x}}^{\beta}\left(\boldsymbol{I}-K^{-1}\mathbf{1}\mathbf{1}^T\right)\left(\boldsymbol{H}_{\boldsymbol{x}}^{\beta}\right)^T \tag{B21}
$$

Taking (B14-16), (B19) and (B21) into (24), yield

$$
\left(\boldsymbol{A}^T\boldsymbol{Q}^{-1}\boldsymbol{A}\right)^{-1}=\mathbf{CRLB\_x} \tag{B22}
$$

So, when the noise level is small, the performance of our proposed algorithm can approximate to the CRLB.

REFERENCES

[1] R. G. Stansfield, "Statistical theory of d.f. fixing," *J. Inst. Elect. Eng.*, vol. 94, no. 15, pp. 762–770, Mar. 1947.
[2] J. Wang, J. Chen, and D. Cabric, "Stansfield localization algorithm: Theoretical analysis and distributed implementation," *IEEE Wireless Commun. Lett.*, vol. 2, no. 3, pp. 327–330, Jun. 2013.
[3] Y. Wang and K. C. Ho, "An asymptotically efficient estimator in closed–form for 3-D AOA localization using a sensor network," *IEEE Trans. Wireless Commun.*, vol. 14, no. 12, pp. 6524–6535, Dec. 2015.
[4] Y. Chan and K. Ho, "A simple and efficient estimator for hyperbolic location," *IEEE Trans. Signal Process.*, vol. 42, no. 8, pp. 1905–1915, Aug. 1994.
[5] H. C. So and L. Lin, "Linear least squares approach for accurate received signal strength based source localization," *IEEE Trans. Signal Process.*, vol. 59, no. 8, pp. 4035–4040, Aug. 2011.
[6] S. Tomic, M. Beko, and R. Dinis, "RSS–based localization in wireless sensor networks using convex relaxation: Noncooperative and cooperative schemes," *IEEE Trans. Veh. Technol.*, vol. 64, no. 5, pp. 2037–2050, May 2015.
[7] S. Yang, G. Wang, Y. Hu, and H. Chen, "Robust differential received signal strength based localization with model parameter errors," *IEEE Signal Process. Lett.*, vol. 25, no. 11, pp. 1740–1744, Nov. 2018.
[8] G. Wang, H. Chen, Y. Li, and M. Jin, "On received-signal-strength based localization with unknown transmit power and path loss exponent," *IEEE Wireless Commun. Lett.*, vol. 1, no. 5, pp. 536–539, Oct. 2012.
[9] Y. T. Chan, F. Chan, W. Read, B. R. Jackson, and B. H. Lee, "Hybrid localization of an emitter by combining angle-of-arrival and received signal strength measurements," in *Proc. IEEE (CCECE)*, Toronto, ON, Canada, May 2014, pp. 1–5.
[10] S. Tomic, M. Beko, and R. Dinis, "3-D target localization in wireless sensor networks using RSS and AoA measurements," *IEEE Trans. Veh. Technol.*, vol. 66, no. 4, pp. 3197–3210, Apr. 2017.
[11] S. Tomic, M. Beko, and R. Dinis, "Distributed RSS–AoA based localization with unknown transmit powers," *IEEE Wireless Commun. Lett.*, vol. 5, no. 4, pp. 392–395, Aug. 2016.
[12] M. Khan, N. Salman, A. Kemp, and L. Mihaylova, "Localisation of sensor nodes with hybrid measurements in wireless sensor networks," *Sensors*, vol. 16, no. 7, p. 1143, Jul. 2016.
[13] S. Chang, Y. Li, X. Yang, H. Wang, W. Hu, and Y. Wu, "A novel localization method based on RSS–AOA combined measurements by using polarized identity," *IEEE Sensors J.*, vol. 19, no. 4, pp. 1463–1470, Feb. 2019.
[14] S. Tomic, M. Beko, and M. Tuba, "A linear estimator for network localization using integrated RSS and AOA measurements," *IEEE Signal Process. Lett.*, vol. 26, no. 3, pp. 405–409, Mar. 2019.
[15] Q. Qi, Y. Li, Y. Wu, Y. Wang, Y. Yue, and X. Wang, "RSS-AOA-based localization via mixed semi–definite and second–order cone relaxation in 3-D wireless sensor networks," *IEEE Access*, vol. 7, pp. 117768–117779, 2019.
[16] S. M. Kay, *Fundamentals of Statistical Signal Processing, Estimation Theory*. Upper Saddle River, NJ, USA: Prentice-Hall, 1993.
[17] G. Golub and C. Van Loan, *Matrix Computations*, 3rd ed. Baltimore, MD, USA: Johns Hopkins Univ. Press, 1996

WANCHUN LI was born in 1978. He received the Ph.D. degree in electronic engineering from the University of Electronic Science and Technology of China (UESTC), in 2009. His research interests include passive localization and electronic countermeasure.

LI WANG was born in Sichuan, China, in 1995. She received the B.S. degree in electronic and information engineering from Southwest University, in 2018. She is currently pursuing the master's degree with the School of Information and Communication Engineering, University of Electronic Science and Technology of China.

MANLIN XIAO was born in Sichuan, China, in 1981. She received the B.Sc. degree in electronics information engineering, the M.Sc. degree in signal and communication engineering, and the D.Sc. degree in signal and information processing from the University of Electronics and Science Technology of China, China, in 2003, 2006, and 2013, respectively. From December 2010 to December 2012, she was a Visiting Scholar with the WINLAB, Rutgers Electrical and Computer Engineering, The State University of New Jersey, USA. She is currently an Assistant Professor with the College of Urban Rail Transportation, Shanghai University of Engineering Science, China. Her major research interests include cognitive radios, synchronization techniques, vehicular communications, and communications in railway transportation.

YINGXIANG LI was born in 1972. He received the Ph.D. degree in electronic engineering from the University of Electronic Science and Technology of China (UESTC), in 2003. His research interests include passive localization and communication theory.

HUAGUO ZHANG received the Ph.D. degree in signal and information processing from the University of Electronic Science and Technology of China, Chengdu, China, in 2011. He is currently an Associate Professor with the School of Information and Communication Engineering, University of Electronic Science and Technology of China. His current research interests include noncooperative communication signal processing and array signal processing.